Proceedings of The Institute of Acoustics

PHASE AND AMPLITUDE FLUCTUATIONS IN A RANDOM MEDIUM

Peter F. Dobbins

British Aerospace
Underwater Research and Engineering Unit, Weymouth, UK.

INTRODUCTION

Predictions of the effect of the random nature of the sea-water medium on beampatterns of sonar transducers require a knowledge of the levels and spatial correlation functions of amplitude and phase fluctuations caused by the random medium [1]. Although a theoretical basis for estimating these parameters has existed for many years, experimental verification is limited. Laboratory experiments have been reported by a number of authors [2-8] but these have concentrated on amplitude fluctuations only. What has been demonstrated is that it is possible to establish a thermal microstructure in a laboratory tank, similar to that found in the ocean, by means of arrays of heating elements at the bottom of the tank.

The experiments described here used this heating technique to generate a random medium in a 3m x 2m x 2m deep laboratory tank. Tonebursts, with frequencies between 70kHz and 160kHz, were transmitted through this random medium and measurements were made of the variance and spatial correlation of both phase and amplitude fluctuations.

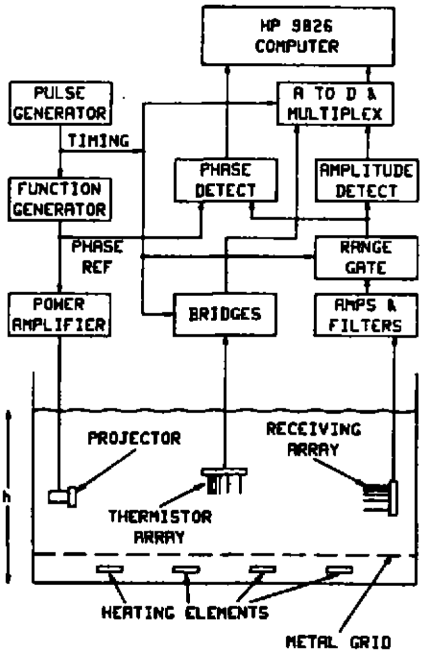

Fig.1 Sketch of experimental set-up.

EXPERIMENTAL EQUIPMENT

The general experimental set-up is shown in Fig.1. An array of 10, 0.65m long, 3kW immersion heaters mounted across the bottom of the tank were used to generate convective currents by heating the water at a constant rate. The power applied to the heaters was limited to 15kW by the laboratory power supply, and could be adjusted by switching between different series and parallel configurations. Perforated metal sheets were mounted above the heaters, to break up the convective currents and encourage the creation of turbulence.

Glass encapsulated thermistors were used to measure the temperature fluctuations, mounted on 15cm long probes fabricated from brass tubing and assembled in an array. Spacings between thermistors in the array were chosen to be compatible with the expected scale size of the thermal structure. For thermal isolation the sensors were separated from the brass tubes by short stalks moulded in epoxy resin.

Two transmitting transducers were used to cover the frequency range. One was a Tonpiltz type, resonant at 70kHz, and the other an air-backed ceramic disc with quarter wave matching, resonant at 120kHz. Both transducers had beamwidths of about 30 degrees at resonance. The receiving transducers were end-capped ceramic cylinders, mounted on probes and assembled in an array identical to the thermistor array except for miniature pre-amplifiers potted along with the electrical connections. These hydrophones had a flat frequency response and were essentially omnidirectional throughout the frequency range of interest.

Each thermistor was connected as one arm of a d.c. bridge which, to avoid self-heating problems, was energised only for a short period (~1μs) when temperature was being sampled. The hydrophone signals, after amplification and filtering, were range gated, allowing discrimination against multipath signals. The amplitude of the signal on each channel was detected by a peak-hold circuit and the phase, relative to a reference derived either from a selected channel or the transmitted signal, was measured by timing between zero crossings of the signal and reference. The phase was obtained directly in digital form, but the amplitude and temperature signals required A to D conversion before the data were passed to an HP 9826 computer for storage and subsequent analysis.

TEMPERATURE MICROSTRUCTURE

The microstructure can be modelled by an empirical one-dimensional spatial wavenumber spectrum, shown in Fig.2, originally formulated by Medwin [9] from measurements in the upper ocean and modified by Chotiros and Smith [7] to suit a laboratory tank. This model is based on the concept that temperature, and hence refractive index, is a passive contaminant of the turbulent water motion. The idealised form of the refractive index spectrum, $\Phi_\mu(\kappa)$ where κ is spatial wavenumber, is outlined by the dashed lines, and is divided into four ranges, separated by the wavenumbers κ_m, κ_t and κ_o.

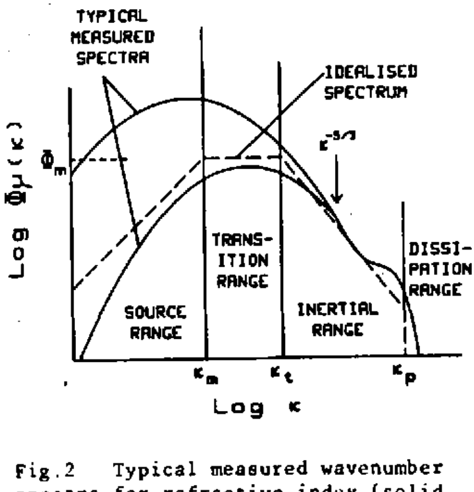

Fig.2 Typical measured wavenumber spectra for refractive index (solid lines) and idealised form (dashes).

Kinetic energy is put into the source range by convection forces; the inertial range contains eddies which obey a five-thirds power law; the transition range is an arbitrary bridge between the source and inertial ranges; in the dissipative range energy is dissipated by viscosity and temperature fluctuations are smoothed by diffusion. It has previously been assumed that the spectrum was truncated below κ_m and above κ_o [7-9]. A detailed description of this model may be found elsewhere [1,7,9] and need not be repeated here.

Preliminary measurements showed considerable variability in the temperature fluctuations in the tank. There were often relatively

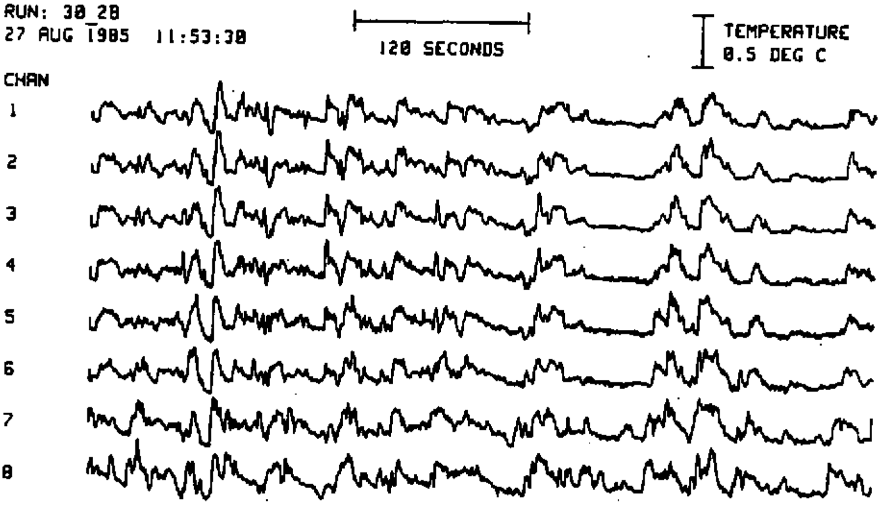

Fig.3 Temperature fluctuation record using the eight thermistor array.

long 'quiet' periods in which the temperature did not fluctuate at all, while at other times the fluctuation level was higher than expected. Although there is no clear-cut explanation of this phenomenon, it has been suggested [10] that swaying of the turbulent plume rising from a heating element could cause the variability. Part of the time the sensor may lie within the plume; part of the time the plume may have swayed off to one side of the sensor; part of the time it may have swayed off to the other side. To counteract this, the spacing between heating elements was reduced so that plumes rising from adjacent elements would overlap and interact. Following this modification the temperature fluctuations were found to be stationary for long periods, and a typical time series record from the eight thermistor array is shown in Fig.3. The overall rms temperature variation in this run was 0.082 deg C which corresponds to a refractive index variation of 1.20 x 10^{-4} rms.

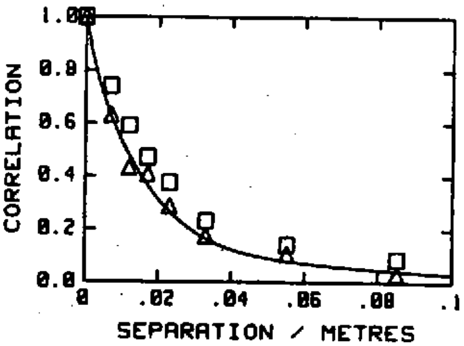

Fig.4 Measured vertical (squares) & horizontal (triangles) temperature spatial correlation coefficients compared with theory (solid line).

Fig.4 shows the cross correlation coefficients between thermistor channel 1 and each of the other channels plotted against separation distance, for runs with the array horizontal (triangles) and vertical (squares) compared with the theoretical spatial correlation function (solid line) obtained by

Fourier transforming the idealised spectrum. Generally the experimental points lie above the theoretical curve. This is because, for simplicity, the source range was excluded from the calculations, but despite this the model gives better over-all agreement with the data than does curve fitting with either Gaussian or exponential curves. The agreement between horizontal and vertical correlations confirms that the thermal microstructure was isotropic.

ACOUSTIC FLUCTUATIONS - THEORY

There exist many theoretical treatments of wave propagation in random media, many of which are reviewed in [11], and the choice of a suitable model for any given application depends upon many factors, the most important being propagation range and frequency, and the scale size and mean square variation of the refractive index inhomogeneities.

These experiments were designed to test Rytov's method (see [11]), because of its wide range of applicability in the ocean. The ultimate limit of validity is somewhat controversial (see eg [12]), but a sufficient set of conditions for this theory is that both the inhomogeneity scale size and the propagation range be large compared with the acoustic wavelength, and that amplitude fluctuations be small. These conditions were satisfied for all experiments.

Formulae for variance, correlation functions and structure functions of phase and log-amplitude for various media are tabulated in [13], and a clear derivation of the fundamental equations is given in [14], so need not be repeated here.

Except for Chotiros and Smith [7], who used very narrow transmitter beams, previous investigators [2-6] have assumed that results for plane wave propagation are applicable, where the basic equation for the spatial correlation functions of log-amplitude, χ, and phase, S, is [14]

$$\left.\begin{matrix} C_\chi(z,r) \\ C_S(z,r) \end{matrix}\right\} = (2\pi k)^2 \int_0^z \int_0^\infty J_0(\kappa r) \left\{\begin{matrix} \sin^2 \\ \cos^2 \end{matrix}\right\} \left[\frac{(z-\eta)}{2k}\kappa^2\right] \kappa \Phi_\mu(\kappa) d\kappa d\eta \qquad (1)$$

where z is propagation range, r is spatial separation, k is the acoustic wavenumber and J_0 is a Bessel function. In this case the integration variable η occurs only in the $\sin^2/\cos^2$ term, so this may be integrated separately giving

$$C(z,r) = 2\pi k^2 z \int_0^\infty J_0(\kappa r) \kappa \Phi_\mu(\kappa) f(\kappa) d\kappa \qquad (2)$$

The function $f(\kappa)$, known as the spectral filter function since it filters a portion of the spectrum Φ_μ, is given by

$$\left.\begin{matrix} f_\chi(\kappa) \\ f_S(\kappa) \end{matrix}\right\} = 1 \mp \sin(\kappa^2 z/k)/(\kappa^2 z/k) \qquad (3)$$

These filter functions are sketched in Fig.5. It is clear that f_χ emphasises the region of Φ_μ above the cut-off wavenumber $\kappa = \sqrt{\pi k/z}$, whilst f_S emphasises the portion below. Thus amplitude fluctuations are affected mostly by small scale inhomogeneities but phase fluctuations depend upon larger scale phenomena. In the past the assumption has been made that if a significant part of the refractive index spectrum is above $\sqrt{\pi k/z}$ then the behaviour of the filter functions near the origin may be ignored, and the approximation

$$f_\chi(\kappa) = f_S(\kappa) = 1 \qquad (4)$$

is valid, the necessary condition normally being expressed as

$$4z/ka^2 \gg 1 \qquad (5)$$

where a is the correlation scale size of the inhomogeneities. The spatial correlation functions then become

$$C_\chi(z,r) = C_S(z,r) = 2\pi^2k^2z\int_0^\infty J_0(\kappa r)\kappa\Phi_\mu(\kappa)d\kappa \quad , \qquad (6)$$

The variances of log-amplitude and phase are found by setting $r = 0$, making the value of the Bessel function unity. Noting the Fourier transform relationship between the refractive index wavenumber spectrum and the associated spatial correlation function, this leads to the well known result

$$\langle\chi^2\rangle = \langle S^2\rangle = \langle\mu^2\rangle k^2za \qquad (7)$$

where $\langle\mu^2\rangle$ is the mean square refractive index variation.

Preliminary experiments showed that although the variance of log-amplitude varied with range and frequency approximately as predicted by Eq.(7), the absolute level was lower than expected. Previous investigators [2-4] have found this and considered that it was due to errors in measuring the thermal microstructure. In the present experiments great care was taken over this measurement and such an explanation is not satisfactory.

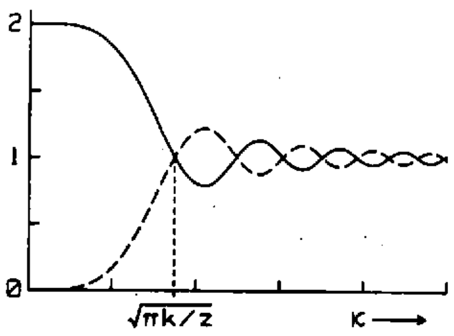

Fig.5 General shape of amplitude (dashes) and phase (solid line) spectral filter functions.

It is known [13] that the theory predicts a lower amplitude fluctuation level when spherical spreading is included. This is done simply by multiplying the distance terms r and $(z - \eta)$ in Eq.(1) by η/z. Unfortunately the simplification in Eqs.(2-7) is no longer possible. For the variance, however, the value of the Bessel function is again unity, and filter functions for spherical spreading can be found for use in Eq.(2), with $r = 0$:

$$\left.\begin{matrix} f_{S\chi}(\kappa) \\ f_{SS}(\kappa) \end{matrix}\right\} = 1 \mp \left(\frac{2\pi k}{\kappa^2 z}\right)^{1/2}\left[\cos\left(\frac{\kappa^2 z}{4k}\right)C\left(\left(\frac{\kappa^2 z}{2\pi k}\right)^{1/2}\right) + \sin\left(\frac{\kappa^2 z}{4k}\right)S\left(\left(\frac{\kappa^2 z}{2\pi k}\right)^{1/2}\right)\right] \qquad (8)$$

where C(x) and S(x) are the Fresnel integrals.

The spherical spreading filters are similar in form to those for plane waves, but the cut-off wavenumber is a factor of $\sqrt{3}$ higher and the oscillations about unity above the cut-off have a higher amplitude and longer period. Although the requirement Eq.(5) was satisfied for the experimental conditions, the cut-off wavenumbers for both plane and spherical filters are higher than the lower limit, κ_m, of the refractive index spectrum. This suggests that the validity condition should be based not on the mean scale size a, which corresponds to the transition wavenumber κ_t, but on the largest scale size, corresponding to κ_m. This new condition necessary for Eq.(7) to be valid may be written

$$4z/ka_o^2 \gg 1 \quad \text{(Plane)}; \qquad 4z/3ka_o^2 \gg 1 \quad \text{(Spherical)} \qquad (9)$$

where a_o is the largest scale present in the refractive index spectrum. This condition was only met in the tank at the lowest frequency and longest range for plane waves, and not at all for spherical waves, so Eq.(7) is not applicable.

EXPERIMENTAL RESULTS

Measured log-amplitude and phase variances are plotted against propagation range in Figs.6A and 6B respectively. These are taken from a number of runs at a frequency of 160kHz and ranges from 0.9m to 2.4m. Because the thermal microstructure changed between runs the results have been normalised by dividing by $<\mu^2>a$. Theoretical predictions using Eq.(7) (solid lines) and Eq.(2) with plane wave (dashes) and spherical wave (dots) filter functions are

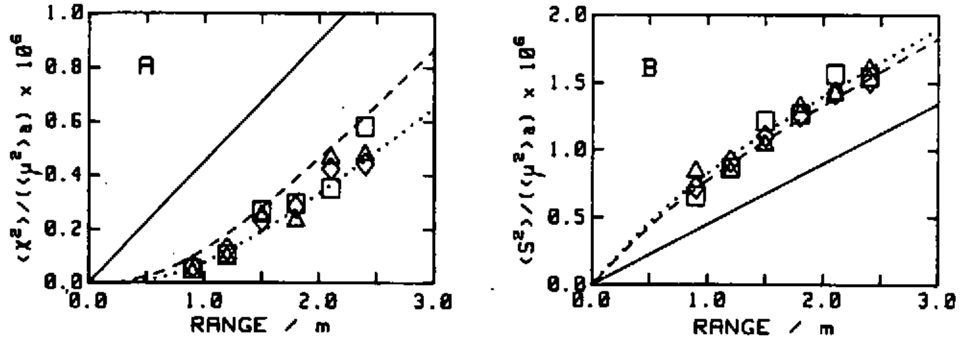

Fig.6 Measured variance of (A) log-amplitude and (B) phase plotted against range and compared with approximate theory (solid lines) and full theory for plane waves (dashes) and spherical spreading (dots).

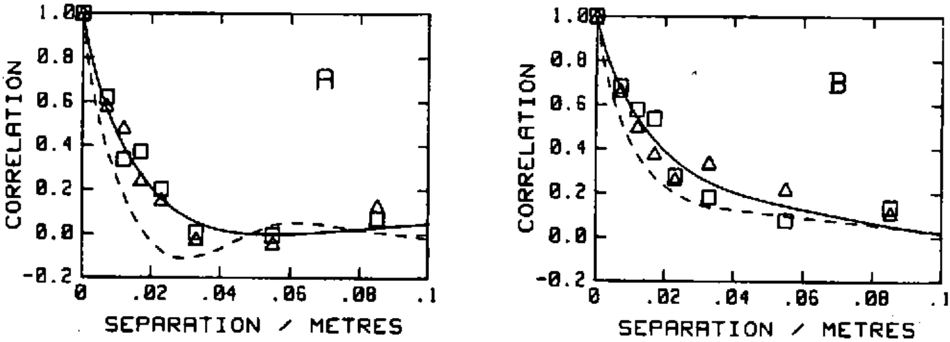

Fig.6 Measured correlation coefficients for (A) log-amplitude and (B) phase plotted against range and compared with approximate theory (solid lines) and full theory for plane waves (dashes) and spherical spreading (dots).

also plotted. It is clear that Eq.(7) grossly overestimates the amplitude fluctuations and underestimates the phase fluctuations. Eq.(2) gives reasonable results for both plane wave and spherical filters, but because of the scatter in the data it is not possible to say with any confidence which gives the better fit.

Figs.7A and 7B show the measured spatial correlations, from the runs at a range of 2.4m for log-amplitude and phase fluctuations respectively. Predictions, from Eq.(2) for plane waves (dashes) and the full double integration, Eq.(1) with r and $(z - \eta)$ multiplied by η/z, for spherical waves (solid lines). For both log-amplitude and phase it is clear that the spherical wave theory gives a better fit to the data, the correlation functions being broader than those for plane waves by a factor of $\sqrt{3}$ in both cases.

CONCLUSIONS

The results presented here show firstly that the simplified expression, Eq.(7), commonly used to estimate the variance of amplitude and phase fluctuations in a random medium must be treated with caution, and that its range of validity depends upon the largest scale of refractive index fluctuation, rather than the mean scale size. Secondly, at least for the conditions applying to these laboratory experiments, spherical wave theory gives a better estimate of the spatial correlation functions of both phase and amplitude fluctuations than the plane wave formulation.

The conditions to be found in the ocean have not been considered here, and it should be noted that the additional computing effort required to apply the spherical wave theory may not be worthwhile if the refractive index fluctuation spectrum is not accurately known. This is particularly true of the low wavenumber end of the spectrum when calculating phase fluctuations and implies that any model of the refractive index structure in the ocean must include large scale phenomena not previously considered necessary for the estimation of amplitude fluctuations only.

ACKNOWLEDGEMENTS

This work was supported by the Procurement Executive, the Ministry of Defence. Thanks are due to Professor H.O. Berktay for helpful comments on the contents of this paper.

REFERENCES

[1] P. Dobbins and C. Schofield, 'Numerical Simulations of the Degradation of Array Directivity due to Scattering', Proc. I.O.A., 7(3), 67-75 (1985)

[2] R.G. Stone and D. Mintzer, 'Range Dependence of Acoustic Fluctuations in a Randomly Inhomogeneous Medium', J.A.S.A., 34(5), 647-653 (1962)

[3] E.O. LaCasce, R.G. Stone and D. Mintzer, 'Frequency Dependence of Acoustic Fluctuationsin a Randomly Inhomogeneous Medium', J. Appl. Phys., 35(9), 2710-2714 (1962)

[4] R.G. Stone and D. Mintzer, 'Transition Regime for Acoustic Fluctuations in a Randomly Inhomogeneous Medium', J.A.S.A., 38, 843-846 (1965)

[5] W.J. Sederowitz and A.G. Favret, 'Covariance between Acoustic Signals Travelling Diverging Paths in a Random Medium', J.A.S.A., 45(2), 386-391 (1969)

[6] S.J. Campanella and A.G. Favret, 'Time Autocorrelation of Sonic Pulses Propagated in a Random Medium', J.A.S.A., 46(5), 1234-1245 (1969)

[7] N.P. Chotiros and B.V. Smith, 'Sound Amplitude Fluctuations due to a Temperature Microstructure', J. Sound Vib., 64(3), 349-369 (1979)

[8] J.W. Posey and C. Levenson, 'High Frequency Propagation through a Turbulent Thermal Plume' (Abstract only), J.A.S.A. Suppl.1, 75, Spring 1984

[9] H. Medwin, 'Sound Phase and Amplitude Fluctuations due to Temperature Microstructure in the Upper Ocean', J.A.S.A., 56(4), 1105-1110 (1974)

[10] A.D. Pierce, 'Analytical Modelling of Random Thermal Fluctuations in the NORDA High Frequency Sound Scattering Facility', NORDA Technical Note 280, July 1984

[11] Yu.N. Barabanenkov, Yu.A. Kratsov, S.M. Rytov and V.I. Tatarskii, 'Status of the Theory of Propagation of Waves in a Randomly Inhomogeneous Medium', Sov. Phys. Uspekhi, 13(5), 551-680 (1971)

[12] D.A. de Wolf, 'Comments on Rytov's Method and Large Fluctuations', J.A.S.A., 54(4), 1109-1110 (1973)

[13] R.S. Lawrence and S.W. Strohbehn, 'A Survey of Clear Air Propagation Effects Relevant to Optical Communication', Proc. IEEE, 58(10), 1523-1545 (1970)

[14] A. Ishimaru, 'Wave Propagation and Scattering in Random Media', Academic Press (1978)